Barrier Properties of Chlorobutyl Nanoclay Composites

V. Sridhar, D. K. Tripathy

Rubber Technology Centre, Indian Institute of Technology, Kharagpur 721302, West Bengal, India

Received 24 April 2005; accepted 16 July 2005
DOI 10.1002/app.22722
Published online in Wiley InterScience (www.interscience.wiley.com).

ABSTRACT: Elastomeric materials are used as barriers to protect workers against exposure to chemicals. The effectiveness of a polymer as a chemical protective material depends on the rate of permeation of chemicals through it. The permeation rate is dependent on the type and amount of fillers added into the polymer matrix. In this study, Chlorobutyl nanoclay composites were prepared by addition of organically modified and unmodified nanoclays at different filler loadings. The nanocomposites were swollen in three solvents of varying cohesive energy density until equilibrium and desorption experiments were carried out. The data obtained from desorption experiments was used to determine the diffusion coefficients. The concentration-dependent diffusion coeffecient (D) was calculated at high and low concentration regions and it was found that D is one-order less in lower concentration region than in the higher concentration range. The aspect ratio of the nanoclay fillers in the composite was calculated by assuming square and disc shapes and it was found to vary with the type of solvent and the used and filler loading. © 2006 Wiley Periodicals, Inc. J Appl Polym Sci 101: 3630–3637, 2006

Key words: rubber; vulcanization; composites

INTRODUCTION

One of the most important applications of elastomeric materials is in the chemical protective clothing (CPC). The effectiveness of a polymer as a chemical protective material therefore depends on the rate of permeation of chemicals through it. The permeation rate depends on the solubility and diffusion coefficient of penetrant in the nanocomposite. Permeation rates can be measured directly by using a permeation cell or they can be calculated from the solubility and diffusion coefficient data. Sorption/desorption experiments can also be used to determine solubility and diffusion coefficients.

Polymer-layered silicate nanocomposites belong to a new class of materials that show promise as barrier materials for a multitude of packaging applications. In recent years, there has been considerable interest in nanocomposites that consist of a polymeric matrix filled with flake-like or plate-like inorganic fillers of high aspect ratio. Incorporation of these nanofillers in polymer matrix is very effective in modifying the mechanical, thermal, and barrier properties as shown by many researchers in a wide variety of polymers including polystyrene,[1,2] polyester,[3] polypropylene,[4–6] polyurathenes,[7] polydimethoxysilane,[8,9] styrene–acrylonitrile copolymers,[10] bromobutyl elastomers,[11] nitrile rubber,[12,13] natural rubber,[14,15] epoxidized natural rubber,[16] etc. Recently, we reported the vulcanization and physicomechanical[17] and dynamic mechanical properties[18] of Chlorobutyl nanocomposites.

The effectiveness of a polymeric material as CPC material depends on its physical properties like tensile strength, elongation, tear resistance, etc. and rate of permeation of chemicals through it.[19] The permeation of penetrant through the polymer matrix depends on penetrant factors like chemical size and shape, polymer factors like type of polymer, its crosslink density, fillers used, etc. and environment variables like temperature, concentration, etc. There are many theories that can correlate solvent diffusivity in polymers. Notable among them are solution–diffusion model, dual mode model, Eyring's hole theory, percolation theory, fractal theory, random walk theory, etc.[20] Solution–diffusion model[21] proposes a three-step process for solvent diffusivity through a polymer matrix: first, the solvent occupies the free volume present in the voids; in the second stage, solvent bounds to the network sites causing swelling; and in the third stage, solvent enters the crosslinked regions. Barrie et al.[21] added one more step by stating that solvent molecules cluster inside the polymer network, which explains the nonlinear isotherm observed for high activity solvents. Aris[22] proposed three mode model of sorption: bulk dissolution of solvent in polymer network, solvent absorption onto the surfaces of vacuoles, which define the excess free volume, and hydrogen bonding between polymer hydrophilic groups and solvents. Chen et al.[23] proposed the diffusion behavior of small molecule penetrants in dense polymer membranes

Correspondence to: D. K. Tripathy (dkt@rtc.iitkgp.ernet.in).

based on percolation theory, fractal theory, and random walk theory. The barrier properties of nanocomposites has been theoretically modeled by many researchers, notable among them being Fredrickson and Bicerano,[24] Cussler et al.,[25] and Bharadwaj.[26]

Theory

When a solvent comes in contact with a polymeric material, the molecules moves through the matrix by diffusion. The one dimensional diffusion process in a membrane is expressed by the following expression:

$$\frac{\partial C}{\partial t} = \frac{\partial}{\partial x}\left(D\frac{\partial C}{\partial x}\right) \tag{1}$$

where D is the diffusion coefficient, C the concentration and t the time. At low concentrations, the above expression reduces to

$$\frac{\partial C}{\partial t} = D\frac{\partial^2 C}{\partial x^2} \tag{2}$$

Under the assumption of uniform concentration of solvent in the matrix, for a plane sheet of thickness l, the above expression can be solved for desorption as

$$\frac{M_t}{M_\infty} = 4\left(\frac{Dt}{l^2}\right)^{1/2}\left[\frac{1}{\pi^{1/2}} + 2\sum_{n=0}^{\infty}(-1)^n ierfc\frac{nl}{2(Dt)^{1/2}}\right] \tag{3}$$

where M_t is the total mass of solvent desorbed at time t and M_∞ is the total mass desorbed at infinite time. Assuming the diffusion process to be Fickian and for small values of t, the above equation reduces to

$$\frac{M_t}{M_\infty} = \left[\frac{16D}{l^2\pi}\right]^{1/2} t^{1/2} \tag{4}$$

Therefore, the slope of the line in plot of M_t/M_∞ vs. $t^{1/2}$ gives us the diffusion coefficient. But, diffusion coefficient is not constant and is concentration dependent. Many studies[19,27] have shown that the initial gradient of desorption gives some mean value for the diffusion coefficient. Therefore, the above expression is rewritten as

$$\frac{M_t}{M_\infty} = \left[\frac{16\bar{D}}{l^2\pi}\right]^{1/2} t^{1/1} \tag{5}$$

where $\bar{D}$ is the average diffusion coefficient in the range of initial concentration C_0 to final concentration (zero). The expression for $\bar{D}$ is given by

$$\bar{D} = \frac{1}{C_0}\int_0^{C_0} D dC \tag{6}$$

Equation (3) can also be written in the following simpler manner

$$\frac{M_t}{M_\infty} = 1 - \frac{8}{\pi^2}\sum_{m=0}^{\infty}\frac{1}{(2m+1)^2}\exp\left[-\frac{D(2m+1)^2\pi^2 t}{l^2}\right] \tag{7}$$

Neglecting all the exponential terms except the first one, at $t = \infty$, the above expression reduces to

$$\frac{M_t}{M_\infty} = 1 - \frac{8}{\pi^2}\exp\left(-\frac{D_0\pi^2 t}{l^2}\right) \tag{8}$$

where D_0 is the diffusion coefficient as concentration of solvent in the matrix approaches zero. Rearranging above expression

$$\ln(M_\infty - M_t) = \ln\left(\frac{8M_\infty}{\pi^2}\right) - \frac{D_0\pi^2 t}{l^2} \tag{9}$$

Therefore, a plot of $\ln(M_\infty - M_0)$ vs. t gives a straight line with slope θ, where

$$\theta = -\frac{D_0\pi^2}{l^2} \tag{10}$$

where D_0 is the diffusion coefficient as concentration approaches zero. The significance of zero concentration diffusivity in polymer systems and its correlation with Cohen-Turnbull-Fujita free volume model was recently reviewed by Hedenquist and Doghieri.[28]

Diffusion coefficient of permeating species is dependent on the concentration and it can be expressed as

$$D = D_0 e^{\beta C} \tag{11}$$

where β is a constant and D_0 is the diffusion coefficient as concentration approaches zero. Substituting in eq. (6) and integrating gives

$$\bar{D} = \frac{D_0}{C_0\beta}[e^{\beta C_0} - 1] \tag{12}$$

In the present work, chlorobutyl nanocomposites were prepared by dispersing organically modified and unmodified montmorillonite nanoparticles at several different clay concentrations (5, 10, and 15 wt %). The nanocomposites are swollen in three different solvents of varying solubility parameters. The solvents used are cyclohexane, chloroform, and trichloroethylene.

TABLE I
Diffusion Coefficient of Cyclohexane in Chlorobutyl Nanoclay Composites

	D^- (10^{-4} cm^2 min^{-1})	D_0 (10^{-3} cm^2 min^{-1})	β
Unfilled	6.31673	4.21335	1.4
Unmodified 5	5.879	5.321	1.84
Unmodified 10	6.2145	5.0214	1.65
Unmodified 15	7.587	5.5698	1.356
Modified 5	3.2458	2.2547	0.854
Modified 10	2.987	2.0547	0.786
Modified 15	4.2369	3.568	0.862

EXPERIMENTAL

Materials

Bayer Chlorobutyl 1240 with 1.25% chlorine content and Mooney viscosity ML_{1+8} at 100°C = 38 were procured from Bayer. Zinc oxide was of chemically pure grade, with specific gravity 5.4. TMTD was supplied by ICI Ltd., Rishra, Hooghly, India, having specific gravity 1.42. Other compounding ingredients like $ZnCl_2$, sulfur, and stearic acid were of chemically pure grade and were procured from standard suppliers. The nanoclays used in this work are sodium montmorillonite and its organically modified counterpart Cloisite 30 purchased from Southern Clay Products, Inc, Texas.

Sample preparation technique

The nanoclays were first heated in vacuum for 12 h at 100°C to remove residual water. These nanoclays were swollen in solvents for 3 days. The rubber was also swollen separately in solvents. The nanoclay and the rubber solutions were then mixed under vigorous stirring. This mixture was allowed to dry for 7 days to remove the solvents. The compounding ingredients (formulation details are in Table I) were added to this rubber–nanoclay mixture on a laboratory size (325 $\times$ 150 mm^2) mixing mill at a friction ratio of 1:1.25, according to ASTM D3182 standards carefully controlling temperature, nip gap, time mixing, and uniform cutting operation. The temperature range for mixing was 65–70°C. The compounded material was molded in an electrically heated hydraulic press to optimum cure (90% of the maximum cure) using molding conditions determined by Monsanto Rheometer (R-100), according to ASTM D2084 and ASTM D5289 procedures.

Swelling measurements

Disc-shaped samples were punched out from the vulcanized sheets using a sharp-edged die. Initially, the samples were dried overnight in a vacuum desiccator, the initial weights were taken, and the thickness was measured within $\pm$0.001 cm at several places with a micrometer screw gauge. Test samples were immersed in solvents in airtight bottles kept at desired temperature in an air oven for 72 h where sorption equilibrium was obtained. Desorption experiments were conducted by exposing the solvent saturated discs to air at 25°C, and the desorption kinetics were monitored by intermittent weighing of the specimen using a Shimadzu AEU balance to the nearest $\pm$0.001 g. At least two desorption experiments were conducted for each sample.

RESULTS AND DISCUSSION

The diffusion coefficient in chlorobutyl nanocomposites as a function of concentration is determined as a function of concentration from D_0 and β. These parameters can be calculated from desorption experiments as follows:

1. $\bar{D}$ is calculated from the slope of linear part of the plots of M_t/M_∞ vs. $t^{1/2}$.
2. D_0 is calculated from the slope of the plots of $\ln(M_\infty - M_t)$ vs. t.
3. β is calculated from eq. (12).

Assuming that no bulk flow exists the permeation flux is estimated by

$$J = -D\frac{\partial C}{\partial X} \tag{13}$$

At steady state, the rate of permeation of solvent can be found by substituting eq. (11) in the above expression:

$$J = \frac{D_0}{\beta l}[e^{\beta C_0} - 1] \tag{14}$$

The results of desorption experiments of unmodified and organically modified montmorillonite filled chlorobutyl vulcanizates plotted as M_t/M_{inf} vs. $t^{1/2}/2l$ in three different solvents viz. cyclohexane, chloroform, and trichloroethylene are shown in Figures 1–6. It is evident that desorption process proceeds quickly in the first few minutes in all the samples. A typical drying curve has three characteristic time periods, an initial transition period, a nearly constant rate period (CRP), and a falling rate period (FRP). Normally, if the solvent is very volatile the initial transition period is not present. In CRP, the rate of solvent desorption is rapid and the rate at which the energy supplied to the system is equal to the rate of energy escaped due to the evaporative cooling occurring during the solvent removal. Most of the solvent is removed during CRP.

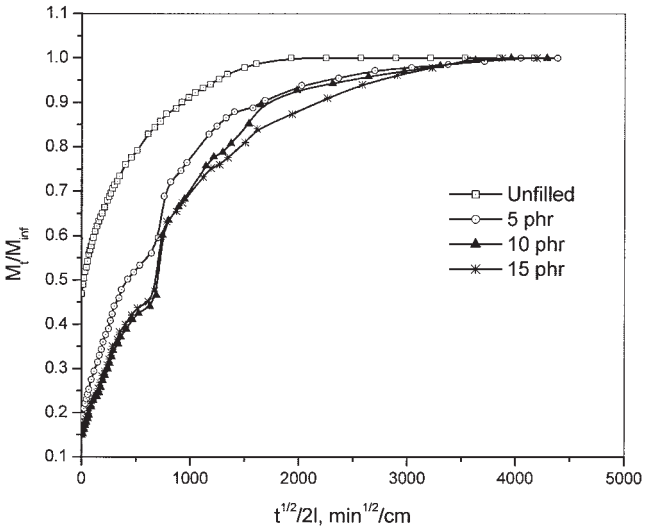

Figure 1 Plot of M_t/M_{inf} vs. $t^{1/2}/2l$ for organically modified montmorillonite filled chlorobutyl vulcanizates in cyclohexane.

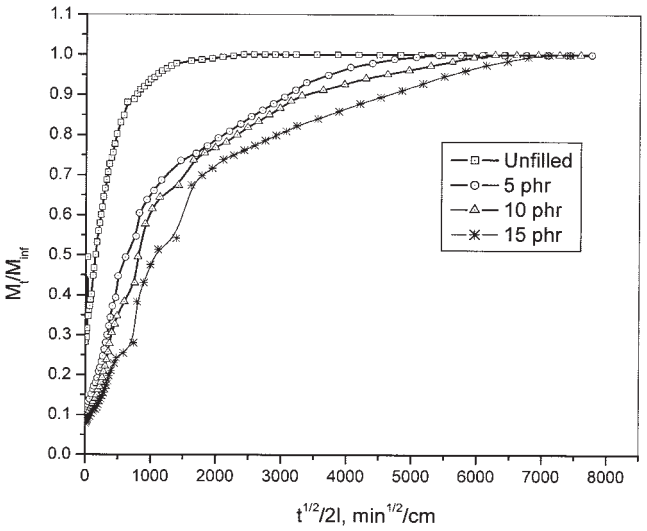

Figure 3 Plot of M_t/M_{inf} vs. $t^{1/2}/2l$ for organically modified montmorillonite filled chlorobutyl vulcanizates in trichloroethylene.

In FRP, the rate of solvent transport to the surface falls due to decrease in solvent content in the vulcanizate, and the rate of solvent transport to the surface from the interiors of the vulcanizate becomes the rate controlling step. In the plateau region, the rate of diffusion of solvent through the vulcanizate decreases still further asymptotically approaching zero. In this region, the resistance to mass transfer comes from the thin solvent depleted layer on the surface of vulcanizate. Desorption behavior of vulcanizates is considered as Fickian diffusion and typical characteristics are summarized below.

- Both uptake and desorption plots of M_t/M_∞ vs. $t^{1/2}/2l$ are initially linear.
- The linear portion generally extends to at least $M_t/M_\infty = 0.6$ for uptake.
- Beyond the linear region, the curves are concave against the abscissa.
- Uptake curves obtained by plotting M_t/M_∞ vs. $t^{1/2}/2l$ should coincide regardless of film thickness.

From Figures 1–6, it is evident that all the vulcanizates regardless of filler loadings and solvents initially show a linear portion, indicating Fickian process. Thereafter, the curves become concave, indicating non-Fickian

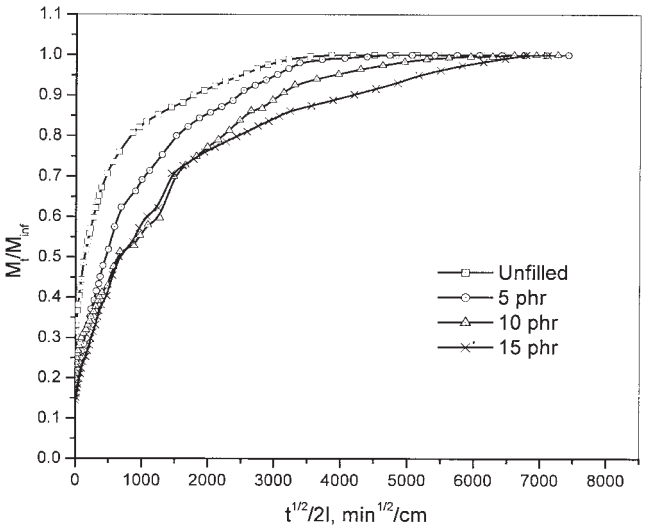

Figure 2 Plot of M_t/M_{inf} vs. $t^{1/2}/2l$ for organically modified montmorillonite filled chlorobutyl vulcanizates in chloroform.

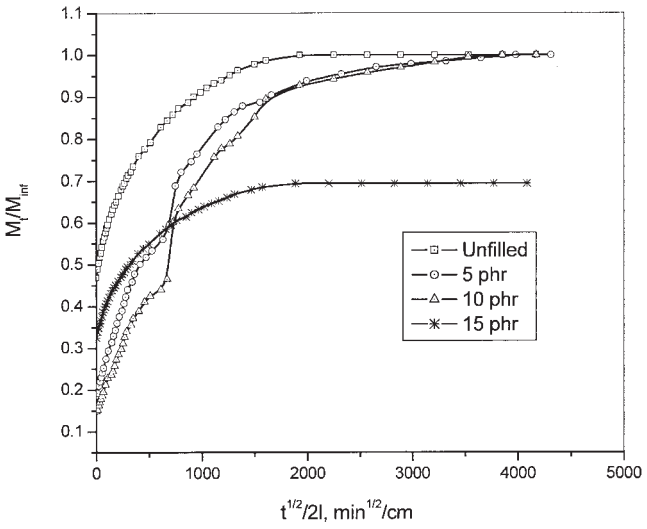

Figure 4 Plot of M_t/M_{inf} vs. $t^{1/2}/2l$ for unmodified montmorillonite filled chlorobutyl vulcanizates in cyclohexane.

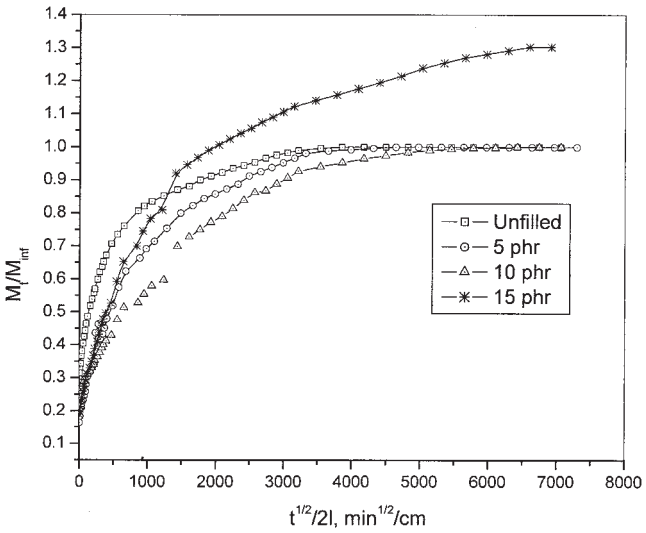

Figure 5 Plot of M_t/M_{inf} vs. $t^{1/2}/2l$ for unmodified montmorillonite filled chlorobutyl vulcanizates in chloroform.

desorption. Minimum of two desorption experiments were performed for each sample. Diffusion coefficients show a maximum in the case of unfilled vulcanizates in all three solvents. From the slopes of linear portion of the curves, diffusion coefficients ($\bar{D}$) for each vulcanizates were calculated and tabulated in Tables I–III. In the case of unmodified montmorillonite nanoclay filled vulcanizates, 15 phr filled samples show highest values of $\bar{D}$. The chemical structure of the clay coating and the resulting interactions with the polymer matrix strongly influences the permeation properties of the nanocomposites. In case of unmodified nanoclay filled Chlorobutyl nanocomposites, the only interactions between the polymer matrix and the

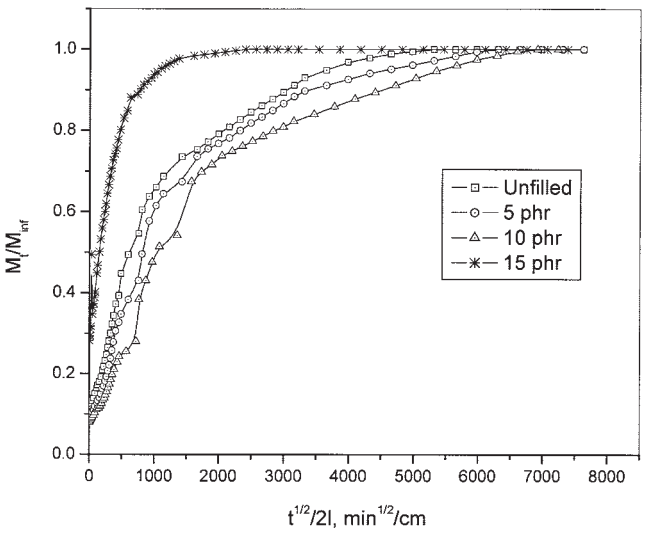

Figure 6 Plot of M_t/M_{inf} vs. $t^{1/2}/2l$ for unmodified montmorillonite filled chlorobutyl vulcanizates in trichloroethylene.

TABLE II
Diffusion Coefficient of TCE in Chlorobutyl Nanoclay Composites

	D^- (10^{-4} cm^2 min^{-1})	D_0 (10^{-3} cm^2 min^{-1})	β
Unfilled	7.3689	3.987	2.1
Unmodified 5	5.832	4.698	2.58
Unmodified 10	8.6358	4.236	3.634
Unmodified 15	9.5621	4.331	2.89
Modified 5	1.5698	0.9658	0.3451
Modified 10	2.0568	1.128	0.5421
Modified 15	2.658	1.354	0.632

clay is mainly due to intercalation and purely physical. With less intercalation occurring within the nanoclay particles, the solvent absorbed within the nanoclusters take more time to desorb. The solvent absorption behavior of montmorillonite nanoclay particles has been well investigated.[29] The organically modified clay is able to swell in organic solvents due to its long alkyl chain modification. Slabaugh and Hiltner[30] showed that *d*-spacing of the alkyl ammonium montmorillonites change when they absorb either polar or nonpolar organic solvents. In the present study, of the three solvents used, cyclohexane desorbs very easily because of its nonpolar nature and its low cohesive energy density (CED). Although TCE being the most polar of all the solvents used, it shows the longest desorption time due to its strong interaction with the vulcanizate because of its higher hydrogen bond. Table IV shows the packing density, diameter, and CED of all the solvents. Papadokostaki et al.[31] based on chemical potential gradients, theoretically showed that the presence of solvents with high affinity with the polymer matrix not only enhance the amount of solvent uptake, but makes desorption more difficult. The dependence of structure of the solvents on the desorption characteristics has been well researched, especially with reference to controlled drug release from polymer monoliths and hydrogels. The transport of penetrants in polymer membranes can be considered to be a process of mixing of polymer and pene-

TABLE III
Diffusion Coefficient of Chloroform in Chlorobutyl Nanoclay Composites

	D^- (10^{-4} cm^2 min^{-1})	D_0 (10^{-3} cm^2 min^{-1})	β
Unfilled	5.601	3.542	2.04
Unmodified 5	3.452	3.021	0.94
Unmodified 10	4.387	3.145	1.65
Unmodified 15	4.895	3.287	1.78
Modified 5	2.5789	1.2563	0.357
Modified 10	2.0254	0.9824	0.4562
Modified 15	2.741	1.1272	0.5381

TABLE IV
Diameter (A^0), Packing Density, and Cohesive Energy Density (CED, Pa) of Solvents Used

	a_β	a_σ	a_w	Y_β	Y	Y_w	ced (10^{-8})
Chloroform	4.72	4.77	5.13	0.410	0.425	0.528	4.13
Trichloro ethylene	4.99	5.07	5.37	0.436	0.455	0.544	3.81
Cyclohexane	5.48	5.36	5.80	0.476	0.446	0.565	3.04

trant molecules accompanied by a creep strain of polymer membrane. Before the solvent gets desorbed, it should come to the surface of the sample. In the case of unmodified nanoclay filled vulcanizates, where the intercalation is less as compared to organically modified nanoclays, desorption occurs much faster as is evident from higher diffusion coefficients (both D_0 and $\bar{D}$). In the case of 5 and 10 phr modified montmorillonite clay loaded vulcanizates, the free chains of the polymer are more intercalated in the nanoparticles, whereas in 15 phr loaded samples, many nanoclay particles are not intercalated and so they will sorb more solvent due to their intrinsic hydrophilic character.

At longer times (i.e., low concentrations of the solvents in the samples), irrespective of the filler or the solvent, the curves become linear. The slope of the linear portion was used to calculate the diffusion coefficient as concentration approaches zero, D_0. In all the cases, the values of D_0 are one-order less than $\bar{D}$. This shows strong dependence of diffusion coefficient on the concentration of the solvent in the vulcanizate. The diffusion coefficient data (both D_0 and $\bar{D}$) was used to calculate the constant β. This equation is nonlinear and was solved with a program developed in MATLAB®. The results are tabulated in the last column of Tables I–III.

The steady state permeation rates of all the solvents have been calculated from eq. (14) and tabulated in Table V. The permeation rates range from 0.32 to 72 μg cm^{-2} s^{-1}. As expected, the vulcanizates with 10 phr modified nanoclay filled nanocomposites show lowest permeation rates. No experimental data has ever been reported for chlorobutyl nanocomposites.

TABLE V
Aspect Ratios and Working Time of Chlorobutyl Nanoclay Composites in TCE

	Aspect ratio		Working time (s)	
	α_{disc}	α_{square}	Disc	Square
Unmodified 5	552	489	148	125
Unmodified 10	447	369	167	134
Unmodified 15	368	174	183	148
Modified 5	1069	948	203	168
Modified 10	863	765	219	179
Modified 15	659	584	238	193

The results show that sorption/desorption experiments can be used to estimate the permeation rates of chemicals through elastomeric nanocomposites. This is an estimation method and as such the results will not be as accurate when compared with permeation cell measurements. But, the sorption/desorption experiments are very simple and require very less material and a few milliliters of challenge chemical. This is an important factor, especially when dealing with potentially carcinogenic VOC (Volatile Organic Chemicals) like trichloroethylene. Chandak et al.[32] reported the VOC sorption behavior of PDMS membranes. They got a diffusion coefficient of 1.44×10^{-6} cm^2 s^{-1}. Our nanocomposites showed diffusion coefficients 2- to 3-fold less than their findings. Sorption/desorption method also provides an expression for calculation of diffusion coefficient at any concentration of the challenge material. Sorption/desorption experiments also provide information about the amount of additives extracted from a polymer during contact with a chemical. Normally, carbon black that is added as filler in conventional vulcanizates is extracted during these type of experiments. But, in the case of nanocomposites made by addition of nanoclays in the polymer matrix, the weight extracted is less than 0.001% of the initial weight. The amount of fillers extracted from a vulcanizate is useful information that industrial hygienists and other professionals can use during CPC material selection.

The other implication of this work is calculation of "working time" or "breakthrough times" that might form a basis for clothing material for soldiers in chemical warfare. The working time for clothing based on ordinary film is given by the expression

$$[\text{Working time}] = \frac{(\textit{film Thickness})^2}{D_0} \qquad (15)$$

For a flake-filled film, the working time will be larger and is expressed by the expression

$$[\text{Working time}] = \frac{(\textit{film Thickness})^2}{D_0} \times \left(1 + \frac{\alpha^2\phi^2}{1-\phi} + \frac{\alpha\phi}{\sigma} + \frac{4\alpha}{\pi(1-\phi)}\ln\left[\frac{\pi\alpha^2\phi}{\sigma(1-\phi)}\right]\right) \qquad (16)$$

where φ is the nanoclay loading, α is the aspect ratio, and $\sigma = \dfrac{\alpha\phi}{1-\phi}$ is the slit width (distance between two

adjacent flakes). Assuming that the nanoclay particles are of disc shape, the aspect ratio α is defined as $\alpha = R/2t$, where t is the thickness of the nanoclay particle. For a dilute concentration of clay in polymer, Fredrickson and Bicerano[33] proposed the following equation

$$\frac{\bar{D}}{\bar{D}_0} = 1 - \frac{\pi}{3}\frac{\alpha\phi}{\ln \alpha} + f(\alpha\phi^2) \tag{17}$$

where $\bar{D}$ and $\bar{D}_0$ are the diffusivities of the nanocomposite and the neat vulcanizate respectively, and φ is the volume fraction of clay in polymer. When the product $\alpha\varphi \ll 1$, the function $f(\alpha\varphi^2)$ can be neglected. Therefore, the aspect ratio can be found by inserting steady state diffusivities and corresponding volume fractions in the above equation. The results of which are tabulated in Table V. Under the assumption of square clay platelets instead of circular discs having the same surface area, the length of platelets would be

$$L_p = \sqrt{\pi R^2} = \sqrt{\pi} R \tag{18}$$

If 2α is the thickness of the platelet, then the aspect ratio can be defined as

$$\alpha_{\text{square}} = \frac{L_p}{2(2\alpha)} = \frac{\sqrt{\pi} R}{2(2\alpha)} = \frac{\sqrt{\pi}}{2}\alpha_{\text{disc}} \tag{19}$$

A model calculation is shown in the Appendix. Converted aspect ratios are shown on the last column of Table V. Using eq. (16), the working time was calculated and tabulated in Table V. Irrespective of solvents, with increase in the nanoclay loading in the composite, there is an increase in working time. But this increase is more pronounced in the case of organically modified nanoclay filled composite than in the unmodified nanoclay loaded ones. This is due to increased interaction between the polymer matrix and the filler.

CONCLUSIONS

Diffusion and permeation characteristics of chlorobutyl nanoclay composites were studied in three solvents of varying cohesive energy densities. Desorption kinetics followed a non-Fickian transport and experimental data was used to calculate the diffusion coefficient as a function of concentration. The results obtained show that the diffusion coefficient is a function of concentration and it is one-order less in lower concentration region than in the higher concentration range. The aspect ratio of the nanoclay fillers was calculated under the assumption that the particles were disc shaped of 1 nm width. The aspect ratio ranged from 369 to 1100, depending upon the type and loading of nanoclay filler. Organically modified clays showed more aspect ratio than their unmodified counterparts. Irrespective of the type of filler, with increasing filler loading, there was a decrease in aspect ratio. The working times calculated show that with increasing filler loading the barrier property of composite increases.

APPENDIX

The density of untreated nanoclay is 2.86 g cm^{-3} as specified by the supplier. Density of vulcanizate without the addition of any filler was determined by water displacement and is 1.136 g cm^{-3}. The organically treated nanoclay contains 29% organic material by weight, found by pyrolysis of the modified clay at 950°C in nitrogen atmosphere. Therefore, 1 g of nanoclay contains 0.29 g of organic matter and 0.71 g of clay.

Basis: *l*00 *g of nanocomposite*

5 *wt % of nanocomposite*

$$= 1.45\ g\ of\ organic\ matter\ +\ 3.55\ g\ of\ clay$$

$$+\ 95\ g\ of\ gum\ vulcanizate\ =\ 1.2413\ cm^3\ \text{clay}$$

$$+\ 83.6267\ \text{cm}^3\ \text{vulcanizate} = 84.868\ \text{cm}^3$$

$$Volume\ fraction\ of\ clay\ (\phi)\ =\ 1.2413/84.868$$

$$= 0.01463$$

Similarly for 10 and 15 phr organically modified nanoclay, the value of ϕ is 0.02926 and 0.04389.

References

1. Vaia, R. A.; Ishii, H.; Giannelis, E. P. Chem Mater 1993, 5, 1694.
2. Giannelis, E. P. Adv Mater (Weinheim, Ger) 1996, 8, 29.
3. Kornmann, X.; Berglund, L. A.; Sterte, J.; Giannelis, E. P. Polym Eng Sci 1998, 38, 1351.
4. Vaia, R. A.; Sauer, B. B.; Tse, O. K.; Giannelis, E. P. J Polym Sci Part B: Polym Phys 1997, 35, 59.
5. Hasegawa, N.; Kawasumi, M.; Kato, M.; Usuki, A. J Appl Polym Sci 1997, 66, 1781.
6. Vu, Y. T.; Rajan, G. S.; Myers, C. L.; Mark, J. E. Polym Prepr (Am Chem Soc Div Polym Chem) 1999, 40, 373.
7. Wang, M. S.; Pinnavia, T. J. Chem Mater 1998, 10, 3769.
8. Burnside, S. D.; Giannelis, E. P. Chem Mater 1995, 7, 1597.
9. Burnside, S. D.; Giannelis, E. P. J Polym Sci Part B: Polym Phys 2000, 38, 1595.
10. Noh, M. H.; Lee, D. C. J Appl Polym Sci 1999, 74, 2811.
11. Burnside, S. D.; Wang, H.-C.; Giannelis, E. P. Chem Mater 1999, 11, 1055.
12. Okada, A.; Fukumori, K.; Usuki, A.; Kojima, Y.; Sato, N.; Kurauchi, T.; Kamigaito, O. Polym Prepr (Am Chem Soc Div Polym Chem) 1991, 32, 540.

13. Kojima, Y.; Fukumori, K.; Usuki, A.; Okada, A.; Kurauchi, T. J Mater Sci Lett 1993, 12, 889.
14. Lopez-Manchado, M. A.; Arroyo, M.; Herroro, B.; Biagiotti, J. J Appl Polym Sci 2003, 89, 1.
15. Joly, S.; Garnaud, R.; Ollitrault, R.; Bokobza, L.; Mark, J. E. Chem Mater 2002, 14, 4202.
16. Vu, Y. T.; Mark, J. E.; Ly, P. H.; Engelhardt, M. J Appl Polym Sci 2001, 82, 1391.
17. Sridhar, V.; Nayak, N. C.; Tripathy, D. K., submitted.
18. Sridhar, V.; Chaudhary, R. N. P.; Tripathy, D. K. J Polym Sci Part B: Polym phys, submitted.
19. Vahdat, N.; Sullivan, V. D. J Appl Polym Sci 2001, 79, 1265.
20. Rogers, C. E. In Polymer Permeability; Comyn, J., Ed.; Elsevier Applied Science: London, 1986.
21. Barrie, J. A.; Vieth, W. R.; Michaelis, A. S. J Appl Phys 1963, 34, 13.
22. Aris, R. Arch Ration Mech Anal 1986, 95, 83.
23. Chen, C.; Han, B.; Li, J.; Shang, T.; Zou, J.; Jiang, W. J Membr Sci 2001, 187, 109.
24. Fredrickson, G. H.; Bicerano, J. J Chem Phys 1999, 110, 2181.
25. Cussler, E. L.; Hughes, W. J; Ward, W. J., III; Aris, J. J Membr Sci 1988, 38, 161.
26. Bharadwaj, R. K. Macromolecules 2001, 34, 9189.
27. Aminabhavi, T. M.; Hemant, T. S.; Phayde, J.; Ortego, D.; Vergnaud, J. M. Polymer 1996, 37, 1677.
28. Hedenquist, M. S.; Doghieri, F. Polymer 2002, 43, 223.
29. Oriakhi, C. O.; Zhang, X.; Lerner, M. M. Appl Clay Sci 1999, 15, 109.
30. Slabaugh, W. H.; Hiltner, P. A. J Phys Chem 1968, 12, 4295.
31. Papadokostaki, K. G. J Appl Polym Sci 2004, 92, 2468.
32. Chandak, M. V.; Lin, Y. S.; Ji, W.; Higgins, R. J. J Appl Polym Sci 1998, 67, 165.
33. Fredrickson, G. H.; Bicerano, J. J Chem Phys 1999, 110, 2181.